

FIGURE 3 The dependence of the steady-state open channel probability ( $p$ ) on membrane potential ( $V$ ). The points are measured as follows: the amplitude histogram of raw single-channel records is fit by two Gaussians centered on the mean open-state current and the mean closed-state current. An event is defined as data points that fall outside 2.56 SD. The time the event occurs is found by extrapolating these points back to the mean. For partial openings (or closings) that do not reach the closed (or open) state, the duration of the event is taken at the moment the data set comprising the event reaches its largest value, or at the moment the data set first reverses the sign of its slope. In this way, an idealized sequence of openings and closings is obtained from the raw data. The points are 0.1 ms apart for data taken at 1,000 Hz bandwidth. The steady-state open-channel probability is the fraction of time spent in the open state between 0.5 and 4.0 s after the voltage step. The figure tests the theoretical curve  $p(V) = 1/1 + \exp(aV + b)$  by comparing the data points to the solid line  $\ln(1/p - 1) = aV + b$  where  $a = -0.0653$  and  $b = -0.871$ . The single time constant from open time histograms depends on voltage according to  $\tau_0 = 11 \exp(V/46)$  ms. The slow component of the closed times obeys  $\tau_c$  (slow) =  $9.2 \exp(-V/22)$  ms. The fast component of the closed times is 13.6 ms at  $-50$  mV and decreases to  $< 0.4$  ms above  $-20$  mV.

rectifier single-channel conductance in heart is four times larger than the K channel conductance found in nerve (5, 6), but the channel density in heart estimated here is  $>1,000$  times lower than in nerve (5). This conclusion depends, of course, on a literal interpretation of the macroscopic data but it seems inescapable that the density of the delayed rectifier channel in heart is extraordinarily low.

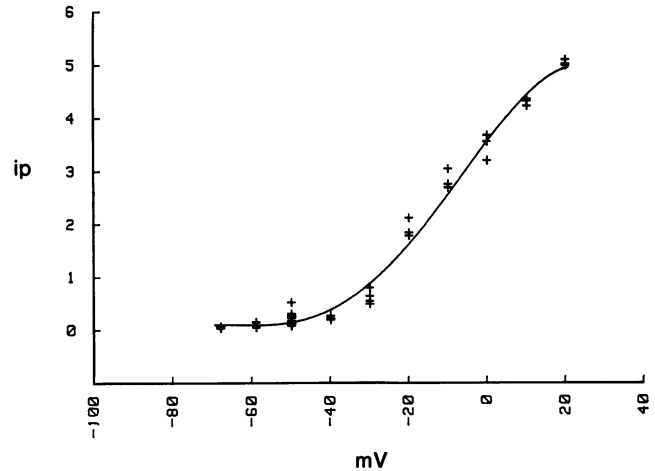


FIGURE 4 The data points are the product of open-channel current ( $i$ ) and the open-channel probability ( $p$ ) vs. membrane potential ( $V$ ). The solid line is the theoretical  $i(V) \cdot p(V)$  relationship, where  $i(V)$  is the solid line fit to the data in Fig. 2 and  $p(V)$  is the theoretical curve taken from Fig. 3. This product is proportional to the macroscopic steady-state  $I(V)$  relationship for this current.

Supported by the Massachusetts Heart Association and the National Institutes of Health grant 1-P01-HL27385.

Received for publication 12 May 1983.

#### REFERENCES

1. Clay, J. R., and A. Shrier. 1981. Analysis of subthreshold pace-maker currents in chick embryo hearts. *J. Physiol. (Lond.)* 312:471-490.
2. Noble, D., and R. W. Tsien. 1969. Outward currents activated in the plateau range of potentials in cardiac Purkinje fibers. *J. Physiol. (Lond.)* 200:205-231.
3. McDonald, T. F., and W. Trautwein. 1978. The K current underlying delayed rectification in cat ventricular muscle. *J. Physiol. (Lond.)* 274:217-246.
4. DiFrancesco, D., A. Noma, and W. Trautwein. 1979. Kinetics of the time-dependent K current in the rabbit SA node. *Pflügers Arch. Eur. J. Physiol.* 381:271-279.
5. Conti, F., L. J. DeFelice, and E. Wanke. 1975. K and Na ion current noise in membrane of the squid giant axon. *J. Physiol. (Lond.)* 248:45-82.
6. Conti, F., and E. Neher. 1980. Single channel recordings of K currents in squid axons. *Nature (Lond.)* 285:140-143.

## SIZE-DEPENDENT KINETICS ASSOCIATED WITH DRUG BLOCK OF SODIUM CURRENT

KENNETH R. COURTNEY

Palo Alto Medical Foundation, Palo Alto, California 94301

#### BASIC MEASUREMENT

Sodium channel block by many drugs is modulated by rate of use of the channel. For instance, rapid trains of action

potentials or depolarizing pulses will enhance channel block to above the basal (resting) level of block. After such conditioning trains, channel block relaxes back to the basal ( $b$ ) level with widely varying time constants ( $T$ ). Sodium

channels in three different preparations are compared here regarding the kinetic rates of unblocking,  $(1 - b)/T$ , after rapid periods of use.

Comparisons of these dose-independent rates of unblocking may provide new information about the micro-environment in and around the sodium channel. These rates, which are intrinsic to different drug structures, are also important because their associated time constants help determine what action potential frequencies an excitable cell can follow during drug treatment. These unblocking rates may also reflect differences in sodium channels in different preparations. The purpose of this presentation is to examine kinetic rates of unblocking in greater detail.

### SIZE/SOLUBILITY HYPOTHESES

Initial studies in nerve suggested that smaller drug structures showed the fastest unblocking kinetics (1). However, small drugs having very poor lipid distribution capabilities, such as procainamide and tocainide, showed anomalously slow rates of unblocking. These rates of channel unblocking may actually represent rates of diffusion away from the sodium channel via a lipophilic pathway (2). Lieb and Stein (3) have suggested a quantitative framework for looking at rates of diffusion through biological membranes as a function of both size and lipid solubility of nonelectrolytes:

$$\log(\text{rate}) = \text{constant} + m \log(\text{mol wt}) - n \log P \quad (1)$$

where  $P$  is the partition coefficient of the diffusing molecule and the parameters  $m$  and  $n$  characterize the size selectivity and solvent power of the membrane. In the application here  $P$  should be replaced by the distribution coefficient  $Q$ , since only the neutral fraction of drug molecules is thought to be capable of rapid intramembrane diffusion. Note that  $Q$  measures the ratio of drug in a model hydrophobic phase (octanol) to total drug in the aqueous phase (see reference 4).

Multiple regression techniques have been used to estimate the  $m$  and  $n$  values in the equation above. Table I summarizes the best-fit parameters for three different preparations. The observation that the solvent power index is  $<1$  suggests that a more hydrophilic membrane solvent than octanol is involved in the diffusion pathway (3).

TABLE I  
SIZE/SOLUBILITY FIT OF UNBLOCKING RATES\*

	$m$	$n$	Goodness of fit
Myelinated nerve	7.4	0.10	$R = 0.92$ (13 drugs)
Skeletal muscle	5.4	0.30	$R = 0.94$ (7 drugs)
Heart muscle	7.7	0.20	$R = 0.94$ (15 drugs)

\*Description of unblocking rate measurement in reference (1) for nerve and (4) for skeletal muscle and myocardium.

Another interpretation of the  $\log Q$  effect is that drugs with lower  $\log Q$  values retain more of their waters of hydration in the diffusion pathway and are, thereby, in effect, larger molecules.

### STEEP SIZE DEPENDENCE

The dependence of unblocking rates on size of the drug is very steep, being inversely related to the seventh power of molecular weight. According to the Stokes-Einstein equation for unrestricted aqueous diffusion, the size dependence of diffusion rate should be much smaller, with the exponent  $m$  (defined above) being between a third and a half. Thus the very steep size dependence observed here may not be explained by models involving free aqueous diffusion, such as unstirred layer effects. Models for diffusion in polymers have been applied to biological situations (3). Such lattice models can successfully explain the steep dependence of these apparent diffusion rates upon molecular size, and suggest that the drug molecule escapes from the channel via a lipophilic pathway.

A cylindrical pore model with a radius of  $\sim 3.6 \text{ \AA}$  would provide another explanation for the dramatic fall in unblocking rates as molecular weights approach 300. This is illustrated in Fig. 1. A similar apparent pore size applies to both myelinated nerve (frog sciatic) and myocardial (guinea pig papillary) preparations. However, absolute unblocking rates are about eight times faster in the warmer ( $35^\circ\text{C}$  vs  $10^\circ\text{C}$ ) myocardial preparations. These pores may represent lattice spaces (3) between the hydrocarbon chains that compose the membrane.

Another possible mechanism for the size-dependence of these unblocking rates should be considered. The slowed repriming of availability of sodium channels with drug

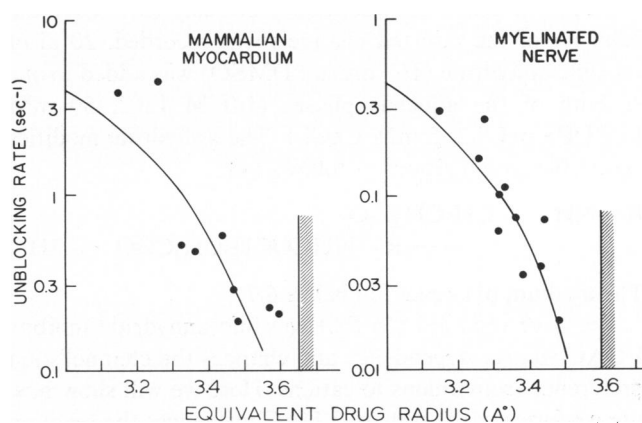


FIGURE 1 Unblocking rates are fit to a cylindrical pore model using the excluded area principle  $[c(r - x)^2]$  where  $r$  is radius of pore and  $x$  is radius of drug. Pore radius  $3.65 \text{ \AA}$  ( $c = 9.5 \text{ s}^{-1}/\text{\AA}^2$ ) fits myocardial observations and  $3.6 \text{ \AA}$  ( $c = 1.2 \text{ s}^{-1}/\text{\AA}^2$ ) fits myelinated nerve measurements. Drugs are treated as equivalent spheres here although they are generally more complex in shape. A molecular weight of 300 corresponds to a molecular volume of about  $180 \text{ \AA}^3$  and an equivalent spherical radius of  $3.5 \text{ \AA}$ .

treatment may actually represent slowed *h*-gating kinetics of drug-altered channels rather than, as suggested above, the rate of drug leaving the channel. In this case different size drugs may promote different repriming kinetics by producing different degrees of stabilization of the closed conformations of *h*-gates.

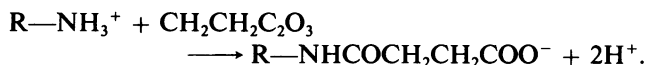
Supported by NIH grants HL24156 and NS15914.

Received for publication 2 May 1983.

## ON THE NATURE OF THE MOLECULAR MECHANISM UNDERLYING THE VOLTAGE DEPENDENCE OF THE CHANNEL-FORMING PROTEIN, VOLTAGE-DEPENDENT ANION-SELECTIVE CHANNEL (VDAC)

CHARLES DORING AND MARCO COLOMBINI  
*Laboratories of Cell Biology*  
*Department of Zoology,*  
*University of Maryland, College Park, Maryland 20742*

We have probed the molecular mechanism underlying the voltage-dependence of the channel-forming protein, voltage dependent anion-selective channel (VDAC) (1). VDAC forms large channels (40 Å in diameter) (2) open at low electric fields and closed at high fields. VDAC, purified from rat liver mitochondria, was introduced into planar phospholipid bilayers by spontaneous insertion from the aqueous phase as described previously (3). After the behavior of the inserted channels was recorded, 20 μl of succinic anhydride (167 mg/ml DMSO) was added to one or both of the aqueous phases (1.0 M LiCl, 50 mM LiMOPS pH 7.2, 5 mM CaCl<sub>2</sub>). The anhydride modifies accessible amino groups as follows (4):



The medium pH never fell below 6.7.

We have reported (5) that succinic anhydride inhibits VDAC voltage dependence and changes the channel's ion preference from anions to cations. Here we will show how the conformational state of VDAC influences the reaction with the anhydride. The results provide clues to the protein's structure, its symmetry, and the location of the gating charges.

### RESULTS

When succinic anhydride was added to membranes containing VDAC in the open state, the channels lost their

### REFERENCES

1. Courtney, K. R. 1980. Structure-activity relations for frequency-dependent sodium channel block in nerve by local anesthetics. *J. Pharmacol. Exp. Ther.* 213:114-119.
2. Hille, B. 1977. Local anesthetics, hydrophilic and hydrophobic pathways for the drug-receptor reaction. *J. Gen. Physiol.* 69:497-515.
3. Lieb, W. R., and W. D. Stein. 1971. The molecular basis of simple diffusion within biological membranes. In *Current Topics in Membrane Transport*. Bonner, editor. Academic Press, Inc., New York. 2:1-39.
4. Courtney, K. R. 1981. Comparative actions of mexiletine on sodium channels in nerve, skeletal and cardiac muscle. *Eur. J. Pharmacol.* 74:9-18.

voltage dependence as measured by the lack of closure in response to an increased field (Fig. 1). A 40-mV voltage difference induced rapid channel closure prior to modification but not after anhydride treatment. (Note that excess anhydride is rapidly destroyed by the water,  $t_{1/2} = 2$  min.) Fig. 2 shows how the voltage dependence is reduced by the modification.

The effects of anhydride modification on VDAC properties when the channel is modified in the closed state depends both on the side of the membrane to which the

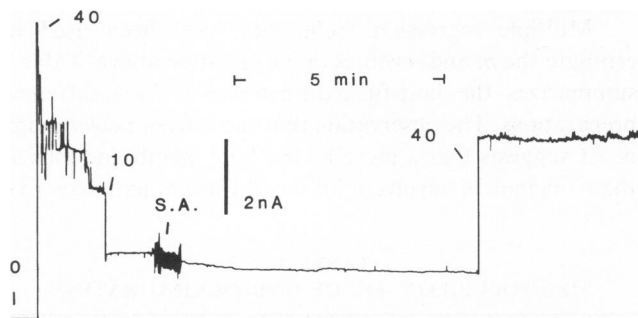


FIGURE 1 Reaction of succinic anhydride with VDAC channels in the open state. VDAC was inserted into planar phospholipid bilayers as described previously (2, 3) and controlled under voltage-clamp conditions. The numbers without units in the figure indicate a change in voltage in millivolts; the sign refers to the *cis* side (the side to which VDAC was added). Succinic anhydride (SA) was added where indicated. The vertical bar indicates 0.2 nA of current.